Redirection of lipid flux toward phospholipids in yeast increases fatty acid turnover and secretion

Raphael Ferreira[a,b,1], Paulo Gonçalves Teixeira[a,b,1], Verena Siewers[a,b], and Jens Nielsen[a,b,c,2]

[a]Department of Biology and Biological Engineering, Chalmers University of Technology, SE412 96 Gothenburg, Sweden; [b]Novo Nordisk Foundation Center for Biosustainability, Chalmers University of Technology, SE412 96 Gothenburg, Sweden; and [c]Novo Nordisk Foundation Center for Biosustainability, Technical University of Denmark, DK2800 Kongens Lyngby, Denmark

Edited by Sang Yup Lee, KAIST, Daejeon, Republic of Korea, and approved December 27, 2017 (received for review August 29, 2017)

Bio-based production of fatty acids and fatty acid-derived products can enable sustainable substitution of petroleum-derived fuels and chemicals. However, developing new microbial cell factories for producing high levels of fatty acids requires extensive engineering of lipid metabolism, a complex and tightly regulated metabolic network. Here we generated a *Saccharomyces cerevisiae* platform strain with a simplified lipid metabolism network with high-level production of free fatty acids (FFAs) due to redirected fatty acid metabolism and reduced feedback regulation. Deletion of the main fatty acid activation genes (the first step in β-oxidation), main storage lipid formation genes, and phosphatidate phosphatase genes resulted in a constrained lipid metabolic network in which fatty acid flux was directed to a large extent toward phospholipids. This resulted in simultaneous increases of phospholipids by up to 2.8-fold and of FFAs by up to 40-fold compared with wild-type levels. Further deletion of phospholipase genes *PLB1* and *PLB2* resulted in a 46% decrease in FFA levels and 105% increase in phospholipid levels, suggesting that phospholipid hydrolysis plays an important role in FFA production when phospholipid levels are increased. The multiple deletion mutant generated allowed for a study of fatty acid dynamics in lipid metabolism and represents a platform strain with interesting properties that provide insight into the future development of lipid-related cell factories.

phospholipids | free fatty acids | *Saccharomyces cerevisiae* | metabolic engineering | CRISPR

Free fatty acids (FFAs) are versatile chemicals that can readily be converted into a broad range of attractive industrial compounds. FFAs are traditionally extracted from plant oils; however, current engineering efforts aimed at creating a more sustainable process are focusing on the development of microbial cells capable of efficiently converting sugars into FFAs (1). With a strong resistance to fermentation inhibitors and an ability to survive at low pH levels, *Saccharomyces cerevisiae* is the preferred cell factory for industrial production of biochemicals (2, 3). It is an extensively well-studied organism with many available genetic tools, such as the CRISPR/Cas9 technology for fast and robust genome editing and pathway interference (4–7). Although the capabilities of *S. cerevisiae* for fatty acid synthesis are limited by strong intrinsic regulations, several attempts have been made to produce FFAs using this organism as a host (8). This increases the importance of understanding the dynamics of lipid metabolism surrounding FFA biosynthesis.

In *S. cerevisiae*, fatty acids are synthesized by the fatty acid synthetase complex encoded by *FAS1* and *FAS2*, in which acetyl-CoA and malonyl-CoA are iteratively processed to produce acyl-CoA. Acyl-CoA formation is tightly regulated through allosteric feedback inhibition of the acetyl-CoA carboxylase Acc1, responsible for malonyl-CoA production (9, 10). Acyl-CoAs from fatty acid biosynthesis are esterified with a hydroxyl-containing molecule (e.g., glycerol or sterol) to form major lipid classes, such as triacylglycerols (TAGs), sterol esters (SEs), or phospholipids. These three lipid classes represent the major pool of fatty acyl chains in *S. cerevisiae*, accounting for most of the total fatty acid-containing lipids in the cell, while other lipid classes are detected only at very low levels (11, 12). In a wild-type cell, FFAs are directly converted to acyl-CoA by fatty acyl-CoA synthetases (13), a process that maintains low FFA levels in the cytoplasm. Previous engineering strategies have shown that deletion of the two dominant acyl-CoA synthetase genes, *FAA1* and *FAA4*, results in deregulation of fatty acid biosynthesis and overaccumulation of FFAs by orders of magnitude above that of a wild-type strain (14–16). Characterization of these strains has indicated that the FFAs originate from complex lipids (14), and as such, are potentially a mere intermediary in lipid hydrolysis and remodeling processes. This effect has been further explored by combining the Δ*faa1* Δ*faa4* genotype with overexpression of the pathway for accumulation and hydrolysis of TAGs (17).

While the foregoing mechanisms have been described and consistently applied in FFA production, to date no studies have properly explored the dynamics of FFA production in the resulting strains in terms of the specific pathways and lipid species involved in FFA formation. Furthermore, during the development of fatty acid-overproducing cell factories, combinatorial effects of modifications regarding fatty acid regulation might come into play, which often are not being properly described or understood in the resulting strains.

Here we developed several strains to study FFA biosynthesis by constraining the lipid metabolic network toward its essential components, i.e., fatty acid and membrane lipid biosynthesis. Analysis of the resulting strains allowed us to understand the role of different lipid pools in FFA formation, as well as the effects of up-regulating phospholipid biosynthesis and the existent relationship between phospholipid and FFA levels in the cell.

Significance

Replacement of nonrenewable petrochemicals and liquid fuels requires sustainable production of oleochemicals. Free fatty acids (FFAs) are versatile molecules that can be produced by microbial fermentation and are used as precursors for production of these oleochemicals. In the past few years, we have seen major advancements in improving the yeast *Saccharomyces cerevisiae* for FFA production. Despite these successes, lipid metabolism is highly complex, and the pathways and metabolites involved in the formation of FFAs in yeast remain incompletely understood. In this work, we make important advancements in understanding the dynamics of FFA formation in the cell and explore the role of phospholipids in this process.

Author contributions: R.F., P.G.T., V.S., and J.N. designed research; R.F. and P.G.T. performed research; R.F. and P.G.T. contributed new reagents/analytic tools; R.F., P.G.T., V.S., and J.N. analyzed data; and R.F. and P.G.T. wrote the paper.

The authors declare no conflict of interest.

This article is a PNAS Direct Submission.

[1]R.F. and P.G.T. contributed equally to this work.

[2]To whom correspondence should be addressed. Email: nielsenj@chalmers.se.

This article contains supporting information online at www.pnas.org/lookup/suppl/doi:10.1073/pnas.1715282115/-/DCSupplemental.

Results

Deletion of Main Acyl-CoA Synthetases and Storage-Lipid Formation Pathways Reveals That FFA Formation Is Independent of Storage Lipids. To construct a strain for studying fatty acid dynamics and fluxes, we removed the two dominant fatty acyl-CoA synthetase-encoding genes, *FAA1* and *FAA4* (Fig. 1), which has been previously shown to be sufficient to abolish FFA reactivation, disrupt the FFA feedback regulation loop, and deregulate fatty acid biosynthesis (13, 18). Removal of these two genes resulted in the RP01 strain that produced 35 mg·gDCW^{1} of FFAs in batch culture (Fig. 2), more than 10-fold compared with the control strain. To prevent FFA and acyl-CoA degradation and provide a more constrained lipid metabolism network, we deleted the fatty acyl-CoA oxidase encoded by *POX1*, which catalyzes the first step of the β-oxidation pathway located in the peroxisomes and is nonessential for growth on glucose (19, 20). *POX1* deletion from the RP01 strain, resulting in strain RP02, led to a 58% increase in produced FFAs, to 53 mg·gDCW^{-1} (Fig. 2).

To investigate the role of neutral lipids in FFA formation, we removed fatty acid accumulation in the form of storage lipids by deleting the two main genes responsible for TAG formation—*DGA1*, encoding diacylglycerol acyltransferase, and *LRO1*, encoding phospholipid:diacylglycerol acyltransferase—and the two main genes responsible for sterol-ester formation—*ARE1* and *ARE2*, encoding acyl-CoA:sterol acyltransferases (Fig. 1). Progressive deletion of the major genes responsible for storage lipid formation resulted in the strain RP09 (*Δfaa1 Δfaa4 Δpox1 Δdga1 Δlro1 Δare1 Δare2*), which did not show significant differences in FFA production levels compared with RP02 (53 mg·gDCW^{-1} and 57 mg·gDCW^{-1}, respectively; $P > 0.05$).

These results suggest that even though storage lipids may have a role in FFA formation, these are not key intermediaries, since RP09 is devoid of TAGs and SEs (Fig. S1) and does not present a major deficiency in FFA formation compared with RP02 (Fig. 2). Even though previous studies have shown that FFAs can be effectively produced using storage lipids as an intermediary (17), our results show that there is an alternative native pathway capable of carrying high fluxes of FFA formation that does not rely on storage lipid synthesis.

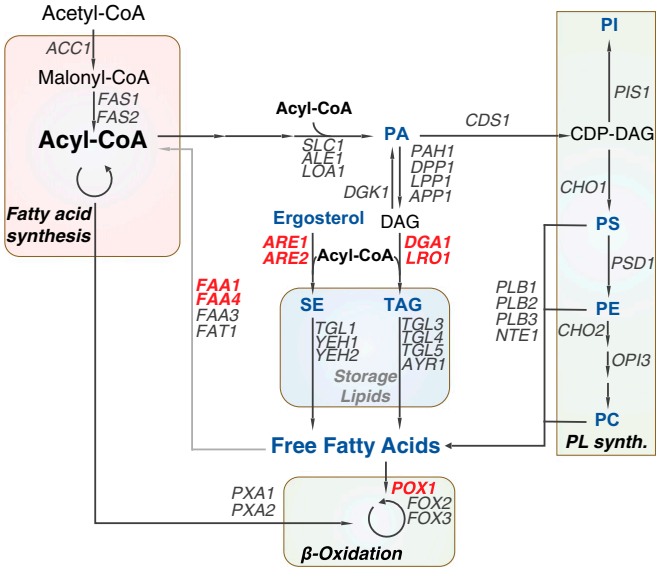

Fig. 1. Simplified schematic representation of key lipid metabolism fluxes and genes in *S. cerevisiae*. Highlighted in red are genes targeted for deletion in the RP09 strain: fatty acyl-CoA synthetases *FAA1* and *FAA4*, fatty acyl-CoA oxidase *POX1*, diacylglycerol acyltransferase *DGA1*, phospholipid:diacylglycerol acyltransferase *LRO1*, and acyl-CoA:sterol acyltransferases *ARE1* and *ARE2*. The lipid species quantified experimentally are in dark blue. PA, phosphatidic acid; PC, phosphatidylcholine; PE, phosphatidylethanolamine; PI, phosphatidylinositol; PL, phospholipids; PS, phosphatidylserine; SE, sterol esters; TAG, triacylglycerols.

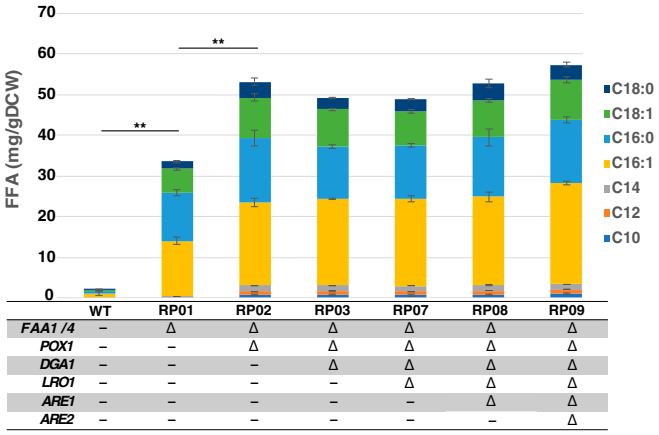

Fig. 2. Effect of disrupting lipid droplet formation on total FFA levels. Total (intracellular and extracellular) FFAs were quantified for the different knockout strains lacking fatty acid reactivation (*FAA1* and *FAA4* deletions), β-oxidation (*POX1* deletion), and storage lipid formation (*DGA1*, *LRO1*, *ARE1*, and *ARE2* deletion). Strains were grown for 72 h in minimal medium containing 2% glucose, and FFAs were quantified from biological triplicates. $^{**}P < 0.005$ (Student's *t* test, two-tailed, two-sample equal variance). Differences between RP03-09 and RP02 were statistically nonsignificant ($P > 0.05$).

Deletion of Phosphatidate Phosphatases Increases the Levels of FFAs and Phospholipids. Use of the strain RP09 allowed for further study of the fatty acid dynamics and pathways involved in FFA formation, since it is devoid of neutral lipids, and thus these could be excluded from the fatty acid pools existent in the cell. According to previous studies, the removal of TAG formation through *DGA1* and *LRO1* deletion leads to an accumulation of diacylglycerols (DAGs) (21). DAGs are formed mainly through dephosphorylation of phosphatidic acid (PA), which is an essential precursor for formation of other phospholipid species. PA has also been characterized as an important signaling molecule for regulation of lipid metabolism. High levels of PA lead to reduced translocation of the transcriptional regulator Opi1 to the nucleus (22), preventing its binding to the transcription factor Ino2. Since Ino2 is an activator of many fatty acid and phospholipid biosynthesis genes, an increase in PA levels indirectly causes an up-regulation of the fatty acid biosynthesis machinery (Fig. 3*B*) (23–25).

To evaluate the effects of up-regulating fatty acid and lipid biosynthesis in this strain and further constrain the network of fatty acid fluxes, we aimed to remove dephosphorylation of PA to DAG (Fig. 3*A*), which would allow for PA accumulation and therefore interfere with Opi1-mediated regulation. PA dephosphorylation is catalyzed by phosphatidate phosphatases encoded mainly by *PAH1*, *LPP1*, and *DPP1*, and as such, these genes were deleted from RP09, resulting in the strain MLM1.0. Deletion of *PAH1*, *LPP1* and *DPP1* led to an increase in total FFAs to 102 mg·gDCW^{-1}, a 98% increase compared with the previous strain RP09 (Fig. 3 *C* and *E*). While levels of both saturated and unsaturated FFAs were increased in MLM1.0, analysis of the FFA composition showed that the percentage of unsaturated (C16:1 and C18:1) compared with saturated (C16:0 and C18:0) FFAs decreased from 62% in RP09 to 56% in MLM1.0. Removal of the phosphatidate phosphatases resulted in exclusive use of PA for phospholipid biosynthesis (Fig. 3*A*) by removing the conversion of PA to DAG. As a result of this flux constraint and the deregulation through PA signaling, phospholipid levels were increased to 30 mg·gDCW^{-1}, an

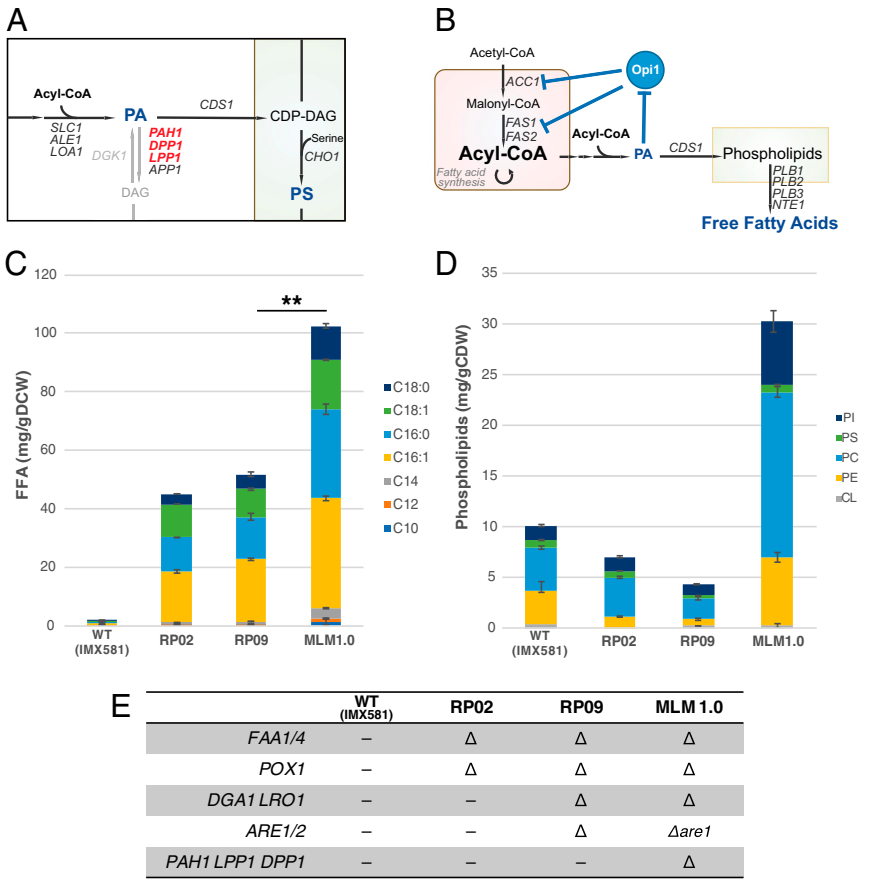

E

	WT (IMX581)	RP02	RP09	MLM 1.0
FAA1/4	–	Δ	Δ	Δ
POX1	–	Δ	Δ	Δ
DGA1 LRO1	–	–	Δ	Δ
ARE1/2	–	–	Δ	*Δare1*
PAH1 LPP1 DPP1	–	–	–	Δ

Fig. 3. Effect of deleting the main phosphatidate phosphatases on the FFA levels. (*A*) Schematic representation of the main reactions forming and consuming PA. Highlighted in red are the genes deleted for removal of phosphatidate phosphatase activity (*PAH1*, *DPP1*, and *LPP1*). (*B*) Signaling mechanism linking PA accumulation and the up-regulation of fatty acid biosynthesis through Opi1. PA binds to Opi1, which indirectly causes an up-regulation of *ACC1*, *FAS1*, and *FAS2* genes. (*C*) Total FFA quantification of MLM1.0 compared with strains RP09, RP02, and the control strain (wt). (*D*) Storage lipid and phospholipid levels in strains RP02, RP09, and MLM1.0 compared with the wild-type control strain. (*D*) Phospholipid levels in strains RP09, MLM1.0, and MLM1.0 + *Δplb1 Δplb2*. PC, phosphatidylcholine; PE, phosphatidylethanolamine; PI, phosphatidylinositol; PS, phosphatidylserine. (*E*) Summary table of genes deleted in each of the evaluated strains. Strains were grown for 72 h in minimal medium containing 2% glucose and all experiments were performed with five biological replicates. ***P* value < 0.005 (Student's *t* test: two-tailed, two-sample equal variance).

eightfold increase compared with RP09 (Fig. 3*D*). The phospholipid fraction was composed mostly of phosphatidylcholine, which accounted for 54% of the total phospholipids, and a similar percentage of phosphatidylethanolamine (PE) and phosphatidylinositol (PI), which accounted for 22% and 21%, respectively. Phosphatidylserine and cardiolipin were present only in low percentages, respectively 2% and 1% of total phospholipids (Fig. 3 *D* and *E*).

Since deregulation of Opi1-controlled phospholipid biosynthesis genes has been previously associated with an expansion of internal ER and nuclear membrane structures (26–28), we performed transmission electron microscopy (TEM) on the main strains, and observed formation of large membrane structures in MLM1.0 that were not observed in the RP02 or RP09 strains (Fig. S2). Furthermore, several stacked membrane sheets were observed in the enlarged ER structure. For strain MLM1.0, aggregates were observed in the medium supernatant after separation of cells by centrifugation. These aggregates could be stained by BODIPY and Nile Red, both fluorescent dyes specific toward lipids (Fig. S3). We speculated that accumulation of phospholipids disturbs membrane formation, ultimately leading to the formation of lipid aggregates in the extracellular medium; however, due to difficulties in isolating these aggregates, extensive characterization could not be carried out. In addition, while not detected in RP09, generation of the strain MLM1.0 resulted in a recurrence of SEs up to 11 mg·gCDW^{-1} in MLM1.0 (Fig. S1). Further investigation through colony PCR indicated incomplete removal of the gene due to the complexity of the genomic region, potentially indicating remaining activity of the *ARE2* gene, and therefore a flux through this enzyme to SE synthesis. Final biomass values for MLM1.0 were decreased compared with the other strains tested. In minimal medium with 2% glucose, MLM1.0 reached biomass values of 5.8 g/L, compared with 6.6 g/L for RP09 and 8.5 g/L for the control strain (Table S1).

Phospholipases B Play a Major Role in FFA Formation in MLM1.0. Through the process of constraining the lipid metabolic network, we observed a simultaneous increase in both phospholipids and FFAs, suggesting the existence of a link between the two lipid groups. Thus, we hypothesized that the FFAs in MLM1.0 are generated mainly through hydrolysis of phospholipids through phospholipases, and that an increased phospholipid content would consequently result in higher FFA levels. The class of phospholipases with a potential role to alter the FFA levels are phospholipases A and B as they cleave the acyl chain at the *sn*-1 and *sn*-2 positions from the glycerol backbone. Phospholipases B are characterized as enzymes that sequentially remove fatty acyl groups at both *sn*-1 and *sn*-2, in contrast to phospholipases A, which cleave uniquely at either *sn*-1 or *sn*-2. Plb1, Plb2, Plb3, and Nte1 are known to exhibit phospholipase B activity (29, 30). As such, we aimed to validate the hypothesis that FFAs are mostly generated from phospholipid hydrolysis

through deletion of the genes encoding the two major phospholipases, *PLB1* and *PLB2* (Fig. 4*A*). This deletion resulted in a decreased level of the total FFA levels by 46%, to 55 mg·gDCW^{-1} (Fig. 4*B*). The percentage of unsaturated FFAs between MLM1.0 and MLM1.0 *Δplb1 Δplb2* decreased from 62% to 40% (Fig. 4*C*), indicating that removal of *PLB1* and *PLB2* hindered the flux of unsaturated FFA formation more than saturated FFA formation. At the same time, these deletions led to an accumulation of total phospholipids up to 61 mg·gDCW^{-1}, a twofold increase compared with MLM1.0 (Fig. 4*D*).

Phospholipid composition changed slightly on deletion of *PLB1* and *PLB2* from MLM1.0; phosphatidylcholine was reduced to 47%, while PI and PS increased to 26% and 4%, respectively. The PE percentage remained the same at 22% of total phospholipids (Fig. 4*E*). This might point toward a higher preference of Plb1 and Plb2 toward PI and PS hydrolysis. The simultaneous decrease in FFA levels and increase in phospholipid levels on deletion of the phospholipase genes *PLB1* and *PLB2* strongly indicates that a significant portion of FFAs in MLM1.0 is generated through phospholipid hydrolysis. Furthermore, previous studies have shown that phospholipids in *S. cerevisiae* mostly incorporate unsaturated fatty acids in both the *sn*-1 and *sn*-2 positions (11), and as such, the decrease in unsaturated FFA supports the hypothesis of FFA formation through phospholipid hydrolysis. Analysis of total fatty acid content in the cell suspension through derivatization of free and bound fatty acids shows similar values of 175 mg·gDCW^{-1} and 180 mg·gDCW^{-1} between MLM1.0 and MLM1.0 Δplb1 Δplb2, respectively, with similar distributions regarding chain length and saturation levels (Fig. S4). These similarities in fatty acid composition while the lipid class distribution is significantly changed (Fig. S1) highly suggest that the fatty acid synthesis machinery is not altered when *PLB1* and *PLB2* are deleted. Here we speculate that it is instead the conversion of phospholipids into other lipid classes, namely FFAs, that is affected. TEM of MLM1.0 *Δplb1 Δplb2* did not show a major difference in accumulation of enlarged intracellular membrane structures; however, we observed that several cells showed a more compact and stacked morphology of these enlarged structures, as opposed to the single large-volume structures observed in MLM1.0 (Fig. S2). This is possibly due to changes in phospholipid composition, such as the change of ratio in saturated to unsaturated fatty acids, which might affect the capability of membrane bending and lead to the formation of particular structures (31, 32).

To investigate whereas Plb1 and Plb2 also play roles in FFA formation in a strain, in which storage lipids and lipid droplets are fully present, and the deregulation of Opi1-controlled phospholipid biosynthesis genes is not applied, we deleted *PLB*1 and *PLB*2 also in the RP02 strain and evaluated the levels of FFAs in that strain. Deletion of both genes resulted in 33 g·gDCW^{-1}, a 20% decrease in FFA levels compared with RP02. This confirms the relevance of phospholipases B in FFA formation and phospholipids as a main precursor for generated FFAs (Fig. S5).

FFA Levels Are Not Affected by Phospholipase Overexpression. Because phospholipid accumulates in MLM1.0 even when high production of FFAs is observed, we wanted to further investigate if FFA formation from phospholipids was limited by phospholipase activity. As such, we individually overexpressed three different phospholipase B genes: *PLB1*, *PLB2*, and *PLB3* (Fig. 5*A*). For this, we used a multicopy plasmid expressing the genes under the control of a strong constitutive *TEF1* promoter. Surprisingly, overexpression of these phospholipases resulted in a maximum increase in total FFA production of only 16% for *PLB2* (*P* values for *PLB1*, *PLB2*, and *PLB3* > 0.05) (Fig. 5*B*). This result suggests that phospholipase activity might not be a major limiting step in FFA production. To further investigate if flux-limiting steps exist elsewhere downstream of acyl-CoA biosynthesis, we expressed a truncated version of the *Escherichia coli* thioesterase gene *tesA* (*'tesA*). Thioesterase overexpression in this strain allows for FFA production directly through the hydrolysis of fatty acyl-CoA. This creates a pathway alternative to the phospholipid-mediated

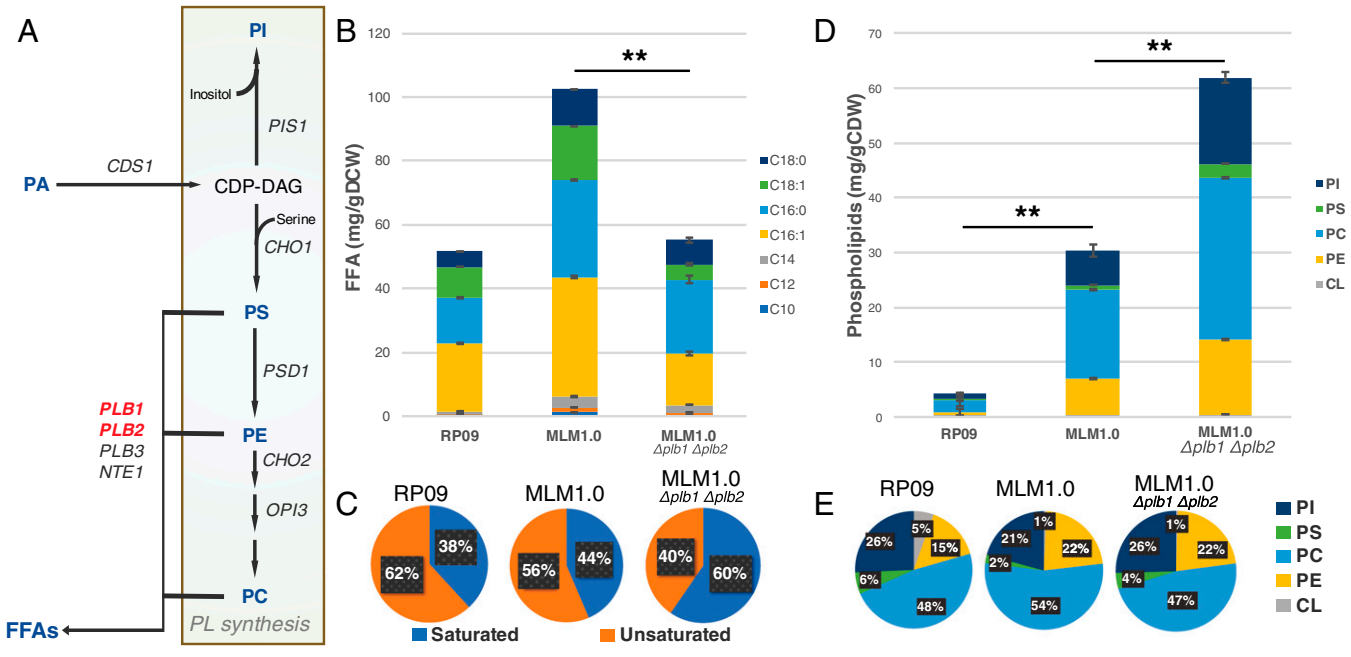

Fig. 4. Effect of deleting phospholipase genes *PLB1* and *PLB2* on FFA production. (*A*) Role of phospholipases B in FFA formation in MLM1.0. Signaled in red are the genes *PLB1* and *PLB2* that were deleted to validate this hypothesis. (*B*) Total FFA quantification of MLM1.0 with *PLB1* and *PLB2* being deleted compared with strains MLM1.0 and RP09. (*C*) Distribution of saturated and unsaturated C16 and C18 FFAs in the three strains. (*D*) Phospholipid levels in strains RP09, MLM1.0 and MLM1.0 + *Δplb1 Δplb2*. PC, phosphatidylcholine; PE, phosphatidylethanolamine; PI, phosphatidylinositol; PS, phosphatidylserine. (*E*) Phospholipid classes distribution in strains RP09, MLM1.0 and MLM1.0 + *Δplb1 Δplb2*. Strains were grown for 72 h in minimal medium containing 2% glucose, FFA and total lipid quantifications were performed with five biological replicates. $^{**}P < 0.005$ (Student's *t* test: two-tailed, two-sample equal variance).

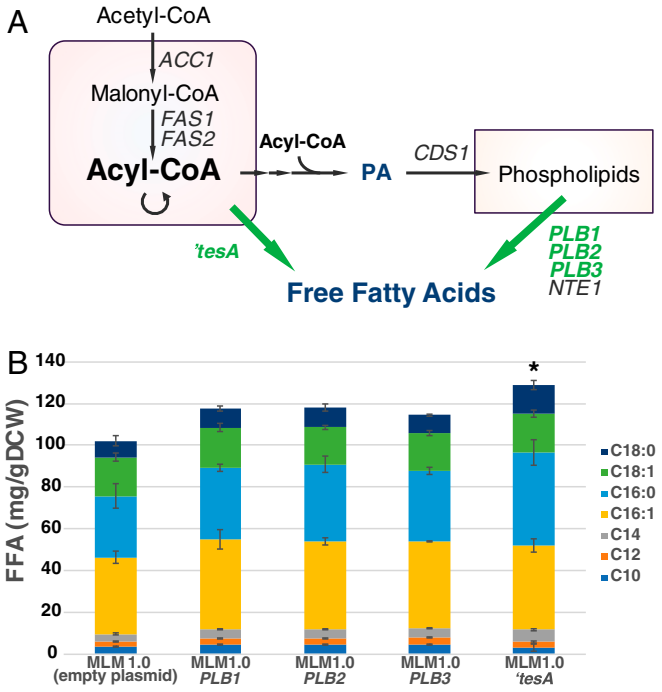

Fig. 5. Effect of overexpressing phospholipase genes *PLB1*, *PLB2*, and *PLB3* and a thioesterase gene *'tesA* in strain MLM1.0. (*A*) Representation of the most significant fatty acid metabolism fluxes in MLM1.0. The genes overexpressed in this experiment are highlighted In green. (*B*) Total FFA quantification of MLM1.0 expressing either phospholipase genes *PLB1*, *PLB2*, *PLB3*, or a thioesterase gene *'tesA* from a 2 μ multicopy plasmid under control of the *TDH3* (*GPD*) promoter. The empty plasmid served as a control. Strains were grown for 72 h in minimal medium containing 2% glucose, and FFA quantification was performed with biological triplicates. $*P < 0.05$ (Student's *t* test; two-tailed, two-sample equal variance). Differences between MLM1.0-PLB1/2/3 and MLM1.0 (empty plasmid) were statistically nonsignificant ($P > 0.05$).

pathway, thereby allowing for production of FFAs independent of the phospholipid production/hydrolysis cycle (Fig. 5*A*). Expression of the thioesterase 'TesA improved FFA production by 26% up to 129 mg·gDCW^{-1} (Fig. 5*B*) with statistical significance ($P < 0.05$). This significant increase in FFA from expression of a thioesterase with expression of phospholipases not resulting in the same increase points toward a flux control at the level of the phospholipid biosynthesis pathway from acyl-CoA rather than a limitation in fatty acid biosynthesis capabilities.

Discussion

Regulating levels of different lipid pools is an evolutionary advantage for a yeast cell, providing the capacity to adapt to different environments or carbon source availability and resistance to stresses. However, as a chassis for cell factory development and metabolic engineering, a complex metabolic network entwined with tight regulation mechanisms can offer many challenges and difficulties for progress. Here we have engineered the lipid metabolism of *S. cerevisiae* by removing many reactions involved in the production of storage lipids, fatty acid oxidation, and conversion of FFAs to fatty acyl-CoA. The combined deletions not only were relevant in reducing the complexity of the metabolic network, but also disrupted several lipid regulation mechanisms. Strains resulting from constraining the lipid metabolic network and redirecting fatty acid fluxes toward phospholipids showed increases in both FFAs and phospholipids, suggesting a strong correlation between the two. Characterization of the resulting strain MLM1.0 points strongly toward phospholipid hydrolysis as a major pathway for FFA formation, identifying phospholipases B as the key players in this process.

The process of deregulating fatty acid and phospholipid biosynthesis genes led to significant changes in the distribution and total levels of most analyzed lipid classes. It also caused severe morphological changes in the internal membrane structure. Taken together, our results highlight the complexity of entwined metabolic and regulatory networks found in *S. cerevisiae* lipid metabolism. By identifying the different factors that come into play and how the lipid species are redistributed in the cell on the redirection of lipid metabolism, we believe to have contributed important information toward understanding the effects that emerge when *S. cerevisiae* is engineered at the level of lipid metabolism.

While the strains developed in this study strongly contribute to fundamental insights into FFAs dynamics, they can also serve as a tool for the development of *S. cerevisiae* as a cell factory for the production of FFAs and fatty-acid derived products. One of the favorable traits of *S. cerevisiae* is its capacity to accumulate high levels of precursors without the tight feedback regulation mechanisms present in lipid metabolism and the lack of major competing reactions for acyl-CoA. Furthermore, the strain was developed through scarless deletions, without the use of resistance markers or other common genetic elements. This offers major advantages for further studies, because it does not limit genome editing options. Along with the advantages of reduced complexity of the lipid metabolic network with improved regulation, the strain also has the benefit of not carrying any overexpression, which means that the strain is not suffering from a protein burden. On the contrary, through the deletion of several genes, it may be possible to allocate proteome mass for the expression of heterologous pathways that further convert the FFAs to other valuable products, such as fatty alcohols, olefins, or alkanes.

Methods

Plasmid Construction and Strain Construction. The plasmids, strains, and primers used in this study are listed in Dataset S1. Oligonucleotides were ordered from Eurofins. All fragments obtained by PCR were gel- or column-purified (GeneJET Gel and PCR Clean-up columns) before cloning, and the resulting plasmids were verified by sequencing (Eurofins). Yeast transformations were performed using lithium acetate and PEG3350 (33). Gene deletions were performed in the strain IMX581 using CRISPR/Cas9 as described previously (34). The diagnostic primers and the repair fragments (listed in Dataset S1) were designed using the Yeastriction webtool (yeastriction.tnw.tudelft.nl/), with the exception of the *PLB1* and *PLB2* deletions, which were carried out with a single gRNA promiscuously targeting both *PLB*1 and *PLB2*, as described previously (35).

Media and Culture Conditions. *S. cerevisiae* strains with auxotrophies were grown on YPD plates containing 20 g·L^{-1} glucose, 10 g·L^{-1} yeast extract, 20 g·L^{-1} peptone from casein, and 20 g·L^{-1} agar. Plasmid-carrying strains were grown on selective growth medium containing 6.9 g·L^{-1} yeast nitrogen base without amino acids (Formedium), 0.77 g·L^{-1} complete supplement mixture without uracil (Formedium), 20 g·L^{-1} glucose, and 20 g· L^{-1} agar. Shake flask cultivations were performed in minimal medium containing 20 g·L^{-1} glucose, 5 g·L^{-1} $(NH_4)_2SO_4$, 14.4 g·L^{-1} KH_2PO_4, and 0.5 g·L^{-1} $MgSO_4{\cdot}7H_2O$. After sterilization, 2 mL·L^{-1} of trace element solution and 1 mL·L^{-1} of vitamin solution were added. The compositions of the trace element and vitamin solution have been reported previously (36). All experiments were performed with strains cultivated as biological replicates, that is, five independent transformants were used to start the precultures.

Quantification of Lipids. Samples for lipid analysis were obtained as 10–15 mL of culture at the end of the shake flask cultivations, after 72 h. Subsequently, the samples were centrifuged at 3,000 × *g* for 5 min, after which the supernatant was discarded. The pellets were kept at −20 °C for 5 min and then freeze-dried in a Christ Alpha 2–4LSC laboratory freeze drier (Christ Gefriertrocknungsanlagen). The samples were analyzed using 10 mg of dried cell biomass as described previously (12).

Quantification of FFAs. FFAs were simultaneously extracted and methylated by dichloromethane containing methyl iodide as a methyl donor (37). In brief, 100-μL aliquots of whole cell culture (cells + supernatant) were placed into glass vials and diluted with 100 μL of water. Then 10 μL 40%

tetrabutylammonium hydroxide (base catalyst) was added, followed immediately by the addition of 200 μL of dichloromethane containing 200 mM methyl iodide as methyl donor and 100 mg·L^{-1} pentadecanoic acid as an internal standard. The mixtures were shaken for 30 min at 1,400 rpm using a vortex mixer, and then centrifuged at 5,000 × *g* to promote phase separation. A 160-μL dichloromethane layer was transferred into a gas chromatography (GC) vial with a glass insert, and then evaporated for 30 min to dryness. The extracted methyl esters were resuspended in 200 μL of hexane and then analyzed by GC (Focus GC; Thermo Fisher Scientific) equipped with a Zebron ZB-5MS capillary column with GUARDIAN (30 m × 0.25 mm × 0.25 μm; Phenomenex) and a flame ionization detector (FID; Thermo Fisher Scientific). The GC program was as follows: initial temperature of 50 °C, hold for 2 min; ramp to 140 °C at a rate of 30 °C/min, then raised to 280 °C at a rate of 10 °C/min and hold for 3 min. The temperature of the inlet was maintained at 280 °C. The injection volume was 1 μL. The flow rate of the carrier gas (helium) was set to 1 mL·min^{-1}. Final quantification was performed using Xcalibur software.

Quantification of Total Fatty Acid Content. Samples for total (bound and free, intracellular and extracellular) fatty acid analysis were taken as 1 mL of culture at the end of 72-h shake flask cultivations. The 1-mL culture volume was kept at −80 °C for 5 min and then freeze-dried in a Christ Alpha 2–4LSC for 3 d. The total lyophilized culture was processed for fatty acid extraction and derivatization to methyl esters as described previously (38). Samples were resuspended in 1 mL of hexane and analyzed with a gas chromatograph (Focus GC; Thermo Fisher Scientific) equipped with a Zebron ZB-5MS capillary column with GUARDIAN (30 m × 0.25 mm × 0.25 μm; Phenomenex) and an FID using the GC program as described previously (38). Final quantification was performed using Xcalibur software.

Lipid Staining. After 72 h of shake flask culture, 100 μL of cell culture was transferred to a 1.5-mL Eppendorf tube, centrifuged, and washed with 1 mL of deionized water. Cells were then centrifuged at 3,000 × *g* for 5 min and resuspended in 100 μL of PBS. Resuspended cells were treated with 1 μL of BODIPY 493/503 solution (1 mg·mL^{-1} in ethanol; Thermo Fisher Scientific), 3 μL Nile Red (1 mg·mL^{-1} in DMSO), or 0.5 μL Calcofluor White M2R (1 mg·mL^{-1} stock solution; Sigma-Aldrich) and kept at 4 °C in the dark for 10 min. Fluorescent microscope pictures were analyzed using a Leica DMI4000B inverted microscope and processed with Leica Application Suite (LAS) software.

TEM. The samples were prepared as described previously 39. In brief, after fixation with glutaraldehyde 2% in cacodylate buffer for 45 min at 4 °C, the yeast cells were treated with Lyticase (Sigma-Aldrich) for 30 min at 37 °C and postfixed with osmium tetroxide 2%, to gently soften the cell wall. Then the samples were dehydrated and embedded in epoxy resin (Agar 100). Ultrathin sections (70 nm) were imaged with a Leo Gemini transmission electron microscope (Zeiss).

ACKNOWLEDGMENTS. We thank Drs. Yongjin Zhou and Michael Gossing for helpful discussions. We acknowledge the Centre for Cellular Imaging at the University of Gothenburg and the National Microscopy Infrastructure (VR-RFI 2016-00968) for providing assistance with microscopy. This project received funding from the Novo Nordisk Foundation, the Knut and Alice Wallenberg Foundation, and the Swedish Foundation for Strategic Research.

1. Nielsen J, et al. (2014) Engineering synergy in biotechnology. *Nat Chem Biol* 10: 319–322.
2. Sheng J, Feng X (2015) Metabolic engineering of yeast to produce fatty acid-derived biofuels: Bottlenecks and solutions. *Front Microbiol* 6:554.
3. Borodina I, Nielsen J (2014) Advances in metabolic engineering of yeast *Saccharomyces cerevisiae* for production of chemicals. *Biotechnol J* 9:609–620.
4. DiCarlo JE, et al. (2013) Genome engineering in *Saccharomyces cerevisiae* using CRISPR-Cas systems. *Nucleic Acids Res* 41:4336–4343.
5. Jakočiūnas T, et al. (2015) Multiplex metabolic pathway engineering using CRISPR/Cas9 in *Saccharomyces cerevisiae*. *Metab Eng* 28:213–222.
6. Zalatan JG, et al. (2015) Engineering complex synthetic transcriptional programs with CRISPR RNA scaffolds. *Cell* 160:339–350.
7. Jensen ED, et al. (2017) Transcriptional reprogramming in yeast using dCas9 and combinatorial gRNA strategies. *Microb Cell Fact* 16:46.
8. Fernandez-Moya R, Da Silva NA (2017) Engineering *Saccharomyces cerevisiae* for high-level synthesis of fatty acids and derived products. *FEMS Yeast Res* 17.
9. Shi S, Chen Y, Siewers V, Nielsen J (2014) Improving production of malonyl coenzyme A-derived metabolites by abolishing Snf1-dependent regulation of Acc1. *MBio* 5: e01130-14.
10. Faergeman NJ, Knudsen J (1997) Role of long-chain fatty acyl-CoA esters in the regulation of metabolism and in cell signalling. *Biochem J* 323:1–12.
11. Ejsing CS, et al. (2009) Global analysis of the yeast lipidome by quantitative shotgun mass spectrometry. *Proc Natl Acad Sci USA* 106:2136–2141.
12. Khoomrung S, et al. (2013) Rapid quantification of yeast lipid using microwave-assisted total lipid extraction and HPLC-CAD. *Anal Chem* 85:4912–4919.
13. Black PN, DiRusso CC (2007) Yeast acyl-CoA synthetases at the crossroads of fatty acid metabolism and regulation. *Biochim Biophys Acta* 1771:286–298.
14. Scharnewski M, Pongdontri P, Mora G, Hoppert M, Fulda M (2008) Mutants of *Saccharomyces cerevisiae* deficient in acyl-CoA synthetases secrete fatty acids due to interrupted fatty acid recycling. *FEBS J* 275:2765–2778.
15. Zhou YJ, et al. (2016) Production of fatty acid-derived oleochemicals and biofuels by synthetic yeast cell factories. *Nat Commun* 7:11709.
16. Teixeira PG, Ferreira R, Zhou YJ, Siewers V, Nielsen J (2017) Dynamic regulation of fatty acid pools for improved production of fatty alcohols in *Saccharomyces cerevisiae*. *Microb Cell Fact* 16:45.
17. Leber C, Polson B, Fernandez-Moya R, Da Silva NA (2015) Overproduction and secretion of free fatty acids through disrupted neutral lipid recycle in *Saccharomyces cerevisiae*. *Metab Eng* 28:54–62.
18. Faergeman NJ, Black PN, Zhao XD, Knudsen J, DiRusso CC (2001) The Acyl-CoA synthetases encoded within FAA1 and FAA4 in *Saccharomyces cerevisiae* function as components of the fatty acid transport system linking import, activation, and intracellular utilization. *J Biol Chem* 276:37051–37059.
19. Sandager L, et al. (2002) Storage lipid synthesis is non-essential in yeast. *J Biol Chem* 277:6478–6482.
20. Valle-Rodríguez JO, Shi S, Siewers V, Nielsen J (2014) Metabolic engineering of *Saccharomyces cerevisiae* for production of fatty acid ethyl esters, an advanced biofuel, by eliminating non-essential fatty acid utilization pathways. *Appl Energy* 115: 226–232.
21. Mora G, Scharnewski M, Fulda M (2012) Neutral lipid metabolism influences phospholipid synthesis and deacylation in *Saccharomyces cerevisiae*. *PLoS One* 7:e49269.
22. Loewen CJR, et al. (2004) Phospholipid metabolism regulated by a transcription factor sensing phosphatidic acid. *Science* 304:1644–1647.
23. Chen X, Yang X, Shen Y, Hou J, Bao X (2017) Increasing malonyl-CoA derived product through controlling the transcription regulators of phospholipid synthesis in *Saccharomyces cerevisiae*. *ACS Synth Biol* 6:905–912.
24. Chen Y, et al. (2016) Improved ethyl caproate production of Chinese liquor yeast by overexpressing fatty acid synthesis genes with OPI1 deletion. *J Ind Microbiol Biotechnol* 43:1261–1270.
25. Kaadige MR, Lopes JM (2006) Analysis of Opi1p repressor mutants. *Curr Genet* 49: 30–38.
26. Santos-Rosa H, Leung J, Grimsey N, Peak-Chew S, Siniossoglou S (2005) The yeast lipin Smp2 couples phospholipid biosynthesis to nuclear membrane growth. *EMBO J* 24: 1931–1941.
27. Han G-S, Siniossoglou S, Carman GM (2007) The cellular functions of the yeast lipin homolog PAH1p are dependent on its phosphatidate phosphatase activity. *J Biol Chem* 282:37026–37035.
28. Adeyo O, et al. (2011) The yeast lipin orthologue Pah1p is important for biogenesis of lipid droplets. *J Cell Biol* 192:1043–1055.
29. Merkel O, et al. (1999) Characterization and function in vivo of two novel phospholipases B/lysophospholipases from *Saccharomyces cerevisiae*. *J Biol Chem* 274: 28121–28127.
30. Fernández-Murray JP, Gaspard GJ, Jesch SA, McMaster CR (2009) NTE1-encoded phosphatidylcholine phospholipase b regulates transcription of phospholipid biosynthetic genes. *J Biol Chem* 284:36034–36046.
31. McMahon HT, Gallop JL (2005) Membrane curvature and mechanisms of dynamic cell membrane remodelling. *Nature* 438:590–596.
32. Szule JA, Fuller NL, Rand RP (2002) The effects of acyl chain length and saturation of diacylglycerols and phosphatidylcholines on membrane monolayer curvature. *Biophys J* 83:977–984.
33. Gietz RD, Schiestl RH (2007) High-efficiency yeast transformation using the LiAc/SS carrier DNA/PEG method. *Nat Protoc* 2:31–34.
34. Mans R, et al. (2015) CRISPR/Cas9: A molecular Swiss army knife for simultaneous introduction of multiple genetic modifications in *Saccharomyces cerevisiae*. *FEMS Yeast Res* 15:1–15.
35. Ferreira R, Gatto F, Nielsen J (2017) Exploiting off-targeting in guide-RNAs for CRISPR systems for simultaneous editing of multiple genes. *FEBS Lett* 591:3288–3295.
36. Verduyn C, Postma E, Scheffers WA, Van Dijken JP (1992) Effect of benzoic acid on metabolic fluxes in yeasts: A continuous-culture study on the regulation of respiration and alcoholic fermentation. *Yeast* 8:501–517.
37. Haushalter RW, et al. (2014) Production of anteiso-branched fatty acids in *Escherichia coli*: next-generation biofuels with improved cold-flow properties. *Metab Eng* 26: 111–118.
38. Khoomrung S, Chumnanpuen P, Jansa-ard S, Nookaew I, Nielsen J (2012) Fast and accurate preparation fatty acid methyl esters by microwave-assisted derivatization in the yeast *Saccharomyces cerevisiae*. *Appl Microbiol Biotechnol* 94:1637–1646.
39. Unger A-K, Geimer S, Harner M, Neupert W, Westermann B (2017) Analysis of yeast mitochondria by electron microscopy. *Mitochondria: Practical Protocols*, eds Mokranjac D, Perocchi F (Springer, New York), pp 293–314.